ISSN 2004-2965 Energy Proceedings, Vol. 24, 2021

International Conference on Applied Energy 2021
Nov. 29 - Dec. 5, 2021, Thailand/Virtual
Paper ID: 390

Pilot Study on Early Warning Systems for Thermal Discomfort Using Body Surface Temperature for Energy Conservation in the Building Sector

Ziyang Wang[1], Ryuji Matsuhashi[1*], Hiroshi Onodera[1]

1 Department of Electrical Engineering and Information Systems, The University of Tokyo, Tokyo, 113-8656, Japan

Email addresses: wang@enesys.t.u-tokyo.ac.jp, matu@enesys.t.u-tokyo.ac.jp, onodera@ee.t.u-tokyo.ac.jp

ABSTRACT

Buildings consume a huge amount of energy and mainly utilize it for occupants' thermal comfort satisfaction. Real-time thermal comfort assessment can enormously contribute to thermal comfort optimization and energy conservation in buildings. Existing thermal comfort models mainly focus on the real-time assessment of occupants' current thermal comfort. However, in the transient thermal environment, occupants' thermal comfort is unsteady and varies from time to time. Therefore, if we only assess occupants' current thermal comfort, prediction error will be elicited. In order to address this problem, it is principally important to comprehend occupants' real-time thermal sensation trend in the transient thermal environment. This study investigates a novel thermal sensation index that can directly represent an individual's current thermal sensation trend. By incorporating the novel thermal sensation index into an ordinary thermal comfort model, a composite thermal comfort model is derived, which can simultaneously address an individuals' current thermal comfort and current thermal sensation trend. Then, by utilizing a machine learning classification algorithm, we propose its intrusive assessment method using skin or clothing temperatures of ten local body parts measured by thermocouple thermometers and its non-intrusive assessment method using a low-cost portable infrared camera. The novel composite thermal comfort model can provide an early warning mechanism for thermal discomfort and contribute to energy conservation in buildings.

Keywords: thermal comfort, energy conservation, physiological index, infrared thermography, machine learning

NOMENCLATURE

Abbreviations	
RTS	Relative Thermal Sensation
3-point RTSS	3-point Relative Thermal Sensation Scale
RTSV	Relative Thermal Sensation Vote
ATS	Absolute Thermal Sensation
7-point ATSS	7-point Absolute Thermal Sensation Scale
ATSV	Absolute Thermal Sensation Vote
3-point TCS	7-point Thermal Comfort Scale
TCL	Thermal Comfort Level
9-point TTCS	9-point Transient Thermal Comfort Scale
TTCL	Transient Thermal Comfort Level
MLP	Multilayer Perceptron
LBPT	Local body part temperatures
DRTP	Dimension-reduced thermal profiles

1. INTRODUCTION

Buildings account directly and indirectly for over one-third of global final energy consumption [1], a large proportion of which (more than 50%) is used for thermal comfort maintenance through the Heating, Ventilation, and Air-conditioning (HVAC) systems. Real-time thermal comfort assessment is not only essential in constructing the control module of the HVAC system but also rather critical in energy conservation in buildings.

Existing thermal comfort models mainly focus on the assessment of occupants' current thermal comfort [2,3]. However, in the transient thermal environment, occupants' current thermal comfort is not stable and varies from time to time [4,5]. For instance, in winter,

Selection and peer-review under responsibility of the scientific committee of the 13th Int. Conf. on Applied Energy (ICAE2021).

suppose an occupant comes back home and turns on the heating system to create a cozy environment. After heating the house for a while, the occupant may feel comfortably warm. Meanwhile, if the power of the heating system is too high, even though the occupant's current thermal comfort is "comfortable," the occupant's thermal sensation may become warmer and warmer. Therefore, it is reasonable to infer that the occupant will likely fall into an uncomfortably hot state if the heating system continues working. In that case, it would be better to lower the power of the heating system in advance to prevent the occupant from running into an uncomfortably hot state. If the occupant's thermal sensation trend can be accurately assessed, not only can thermal discomfort be predicted in advance, but energy can also be saved.

In order to address this concern, in this paper, we present a composite thermal comfort model by introducing a novel thermal sensation index into an ordinary thermal comfort model.

2. METHODOLOGY

2.1 Relative Thermal Sensation

In this study, the thermal sensation is considered to be a first-order differentiable function $f(t)$ of time t, where $f(t)>0$ denotes hot sensation, $f(t)<0$ denotes cold sensation, $f(t)=0$ denotes neutral sensation. The larger its absolute value $|f(t)|$, the greater the degree of hotness or coldness. The first-order derivative of $f(t)$, describing the trend of the thermal sensation, is precisely defined as the Relative Thermal Sensation (RTS) in this study. Next, the 3-point Relative Thermal Sensation Scale (3-point RTSS) is defined to be discrete and consists of three categories "hotter" (+1), "no change" (0), and "colder" (-1), each category in which is called a Relative Thermal Sensation Vote (RTSV). The RTSV is defined as "hotter" when the occupant is currently feeling hotter than the latest thermal sensation ($f'(t)>0$); the RTSV is defined as "colder" when the occupant is currently feeling colder than the latest thermal sensation ($f'(t)<0$); when the occupant's current thermal sensation does not change compared with the latest thermal sensation (neither "hotter" nor "colder," when $f'(t)=0$), the RTSV is defined as "no change." By such a definition, the RTS forms another dimension of thermal comfort, and it can serve as a complementary thermal sensation index for traditional thermal comfort models.

2.2 Composite thermal comfort model

In this study, to better distinguish from the RTS and the 3-point RTSS, we denominated the thermal sensation in the common sense as the Absolute Thermal Sensation (ATS). By such a definition, the thermal sensation is decomposed into two categories: ATS and RTS. Moreover, we define the 7-point Absolute Thermal Sensation Scale (7-point ATSS) consists of seven categories "very cold" (-3), "cold" (-2), "cool" (-1), "neutral" (0), "warm" (+1), "hot" (+2), and "very hot" (+3), each category in which is called an Absolute Thermal Sensation Vote (ATSV). In the 7-point ATSS, the "cool," "neutral," and "warm" votes are defined to represent comfortable sensations; the "hot" and "very hot" votes are defined to represent uncomfortably hot sensations; the "cold" and "very cold" votes are defined to represent uncomfortably cold sensations. Consequently, the 3-point Thermal Comfort Scale (3-point TCS) can be derived from the 7-point ATSS. The 3-point TCS has three categories "hot" (+3), "cozy" (0), and "cold" (-3), each category in which is called a Thermal Comfort Level (TCL).

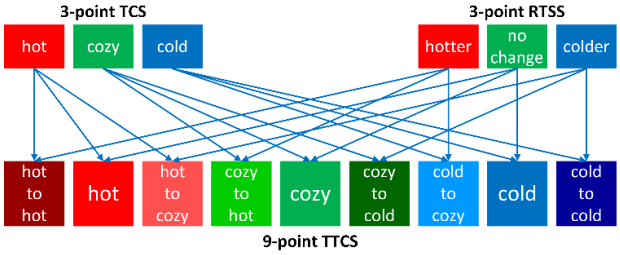

Fig. 1 9-point TTCS by incorporating the 3-point RTSS into the 3-point TCS

By incorporating the 3-point RTSS into the 3-point TCS (combine each category in the 3-point RTSS with each category in the 3-point TCS), we can obtain the 9-point Transient Thermal Comfort Scale (9-point TTCS), which is a composite real-time thermal comfort model and can describe an individual's current thermal comfort and current thermal sensation trend simultaneously, as described in Fig. 1. The 9-point TTCS has nine categories "hot to hot" (+4), "hot" (+3), "hot to cozy" (+2), "cozy to hot" (+1), "cozy" (0), "cozy to cold" (-1), "cold to cozy" (-2), "cold" (-3), "cold to cold" (-4), each category in which is called a Transient Thermal Comfort Level (TTCL).

In the 9-point TTCS, the "hot to hot" and "cold to cold" TTCLs indicate an individual's hot or cold discomfort degree will aggravate in the future; the "hot to cozy" and "cold to cozy" TTCLs indicate an individual's hot or cold discomfort degree will alleviate in the future;

the "cozy to hot" and "cozy to cold" TTCLs indicate an individual tends to feel uncomfortably hot or cold in the future.

2.3 Novel thermal sensation voting system

The subjects were requested to input the real-time ATSVs and RTSVs through a laptop. The number keys "1," "2," "3," "4," "5," "6," and "7" correspond to the ATSVs "very cold," "cold," "cool," "neutral," "warm," "hot," and "very hot," respectively. The arrow keys "up" and "down" correspond to the RTSVs "hotter" and "colder," respectively, as illustrated in Fig. 2. The subjects should input either the ATSV or RTSV at least once when hearing an alarm that rings every 20 sec. The priority of the ATSV is higher than the RTSV. Moreover, in order to gather as many thermal sensation details as possible, the subjects were encouraged to input the ATSV and RTSV whenever they felt a change in their thermal sensation. The "hotter" and "colder" RTSVs were regarded to sustain 20

Fig. 2 Keyboard layout for ATSV and RTSV input

sec after the input when there is no successive "hotter" or "colder" RTSV within 20 sec. The "no change" RTSV was not set as an active vote to alleviate the mental burden. Time periods with no "hotter" or "colder" RTS were regarded as the "no change" RTS periods.

2.4 Intrusive and non-intrusive body surface temperature measuring methods

As is known to all, intuitively, people tend to feel hotter when the air temperature is ascending, while they tend to feel colder when the air temperature is descending. However, the real-time RTS could be much more complicated than simply judging by the air temperature. We hypothesized that it is possible to assess the RTS by analyzing the body surface temperatures of several local body parts or the thermal images of the body surface. We measured the local body part temperatures (LBPT) of ten locations, including the forehead, the upper chest, the lateral arm, the dorsum of the hand, the abdomen, the scapular blade, the anterior thigh, the fibular shin, the posterior wrist, and the dorsum of the foot in an intrusive way using thermocouple thermometers (Accuracy: ±0.5℃). Also, we utilized a low-cost portable infrared camera FLIR ONE Pro ($375) to cover the subjects' upper body surface infrared radiation in a non-intrusive manner. Both the LBPT and the thermal images were taken per sec.

2.5 Feature extraction and feature engineering for RTS and TCL assessments by classification algorithm

We used an instance segmentation algorithm (YOLACT++ [6]) to remove the background surrounding the subjects' thermal profiles in the thermal images and applied dimensionality reduction to the background-removed thermal profiles using the UMAP [7] to perform feature extraction and obtain the dimension-reduced thermal profiles (DRTP) (from 160×120 to 10). Then, we used the LBPT and the DRTP for personal TCL modeling, separately. Since the RTS is the gradient of the ATS, reasonably, we used the LBPT and the gradients of LBPT as well as the DRTP and the gradients of DRTP for personal RTS modeling, separately. Five-fold blocked cross-validation was carried out to predict personal RTS and TCL using the Multilayer Perceptron (MLP) classifier since the data have time dependencies according to [8]. Optimal hyper-parameters were obtained using the grid

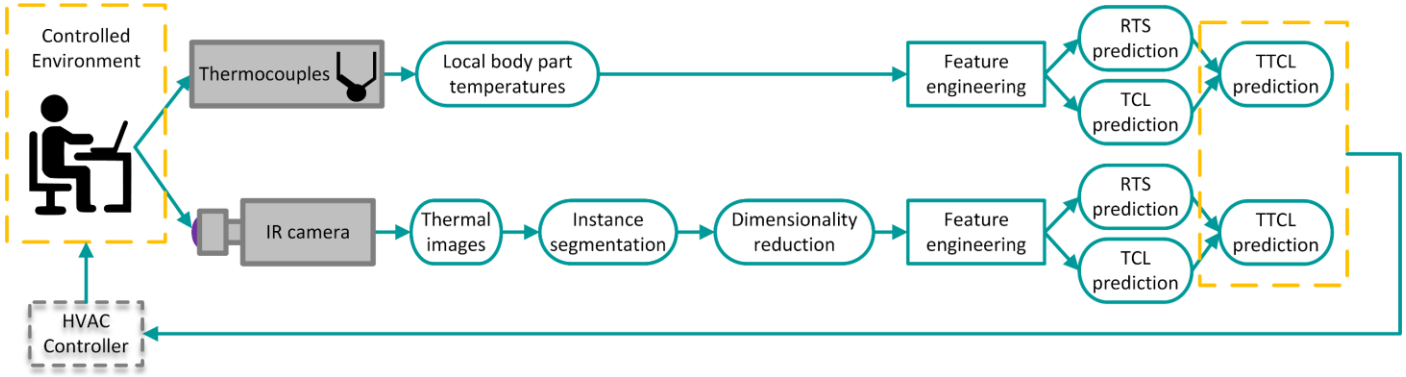

Fig. 3 Overview of the proposed individual TTCL assessment framework for an occupant-centered HVAC control system.

search technique. Fig. 3 illustrates the TTCL assessment framework using the above-mentioned intrusive and non-intrusive methods for an occupant-centered HVAC control system.

3. EXPERIMENTAL SETUP

The experiment was conducted in the environmental test lab of Tokyo Gas Co., Ltd, which consists of an external environment and an inner chamber, as illustrated in Fig. 4. Six male students (age 25 ± 1 years) at the University of Tokyo participated in the experiment. By various operations of the HVAC system and the door, two Scenarios were created to test the RTS and ATS performance under such thermal conditions, as illustrated in Fig. 6. Three subjects were randomly selected and dispatched to Scenario I, and the other three were dispatched to Scenario II.

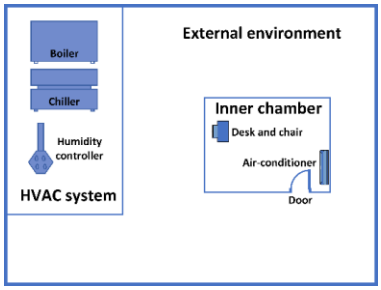

Fig. 4 Schematic of the environmental test lab.

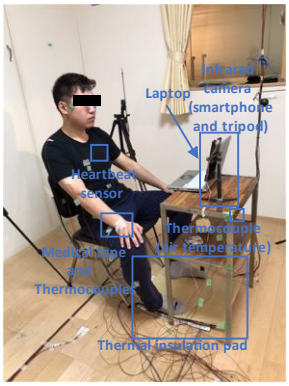

Fig. 5 A male subject and the mounting state of the experimental apparatus.

A laptop for ATSV and RTSV input was set on a desk in front of a chair. The desk and the chair were arranged not to directly face the airflow from the air-conditioner of the door, as illustrated in Fig. 4. The subjects were requested to wear the same clothes provided by us (black short sleeves, trousers, and cotton socks), sit down on the chair, and press the keyboard buttons to input the ATSV and RTSV during the experiment to simulate sedentary office activities (small range of motion allowed), as shown in Fig. 5.

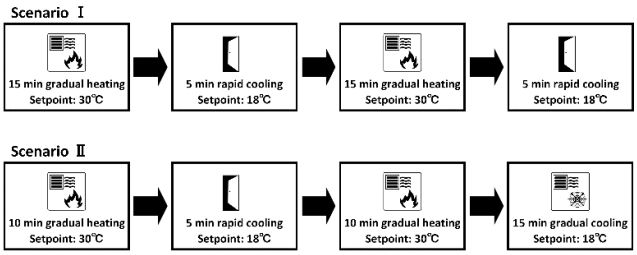

Fig. 6 Temperature control schemes of the inner chamber.

4. RESULTS AND DISCUSSION

4.1 Visualization of the LBPT, DRTP, RTSVs and ATSVs

Fig. 7 and Fig. 8 show the representative data of two subjects from Scenarios I and II, respectively. In both Fig. 7 and Fig. 8, during "hotter" periods, the shin temperature is higher than the abdomen temperature,

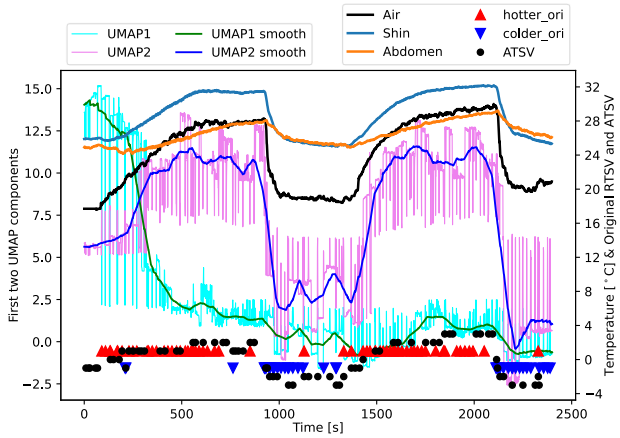

Fig. 7 Shin, abdomen, and air temperatures, original ATSVs and RTSVs, first two UMAP components, and smoothed first two UMAP components (Scenario I & subject 1).

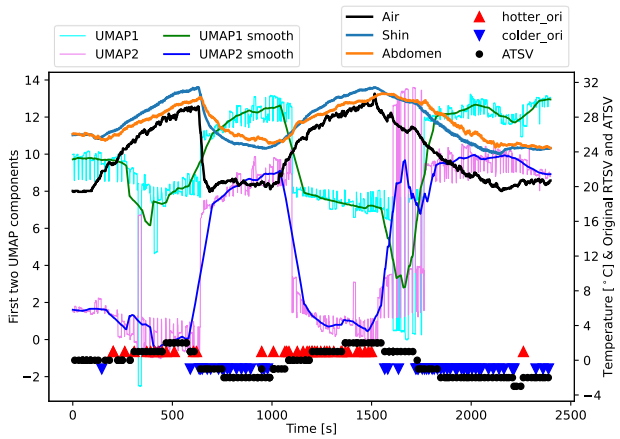

Fig. 8 Shin, abdomen, and air temperatures, original ATSVs and RTSVs, first two UMAP components, and smoothed first two UMAP components (Scenario II & subject 4).

whereas during "colder" periods, the shin temperature is lower than the abdomen temperature, indicating that it could be reasonable to use the LBPT for RTS modeling. During "hotter" periods, the shin and abdomen temperatures tend to be ascending, whereas during "colder" periods, they tend to be descending, indicating that it could be reasonable to use the gradients of the LBPT for RTS modeling. For the DRTP, in Fig. 8, during "hotter" periods, the smoothed first two UMAP components occupy lower ranges; during "colder" periods, they occupy higher ranges. In Fig. 7, during "hotter" periods, the second smoothed UMAP component occupies a higher range and occupies a lower range during "colder" periods, indicating that it could be reasonable to use the DRTP for RTS modeling. However, different from the LBPT, the first smoothed UMAP component in Fig. 7 does not satisfy this pattern since the UMAP is a non-linear process.

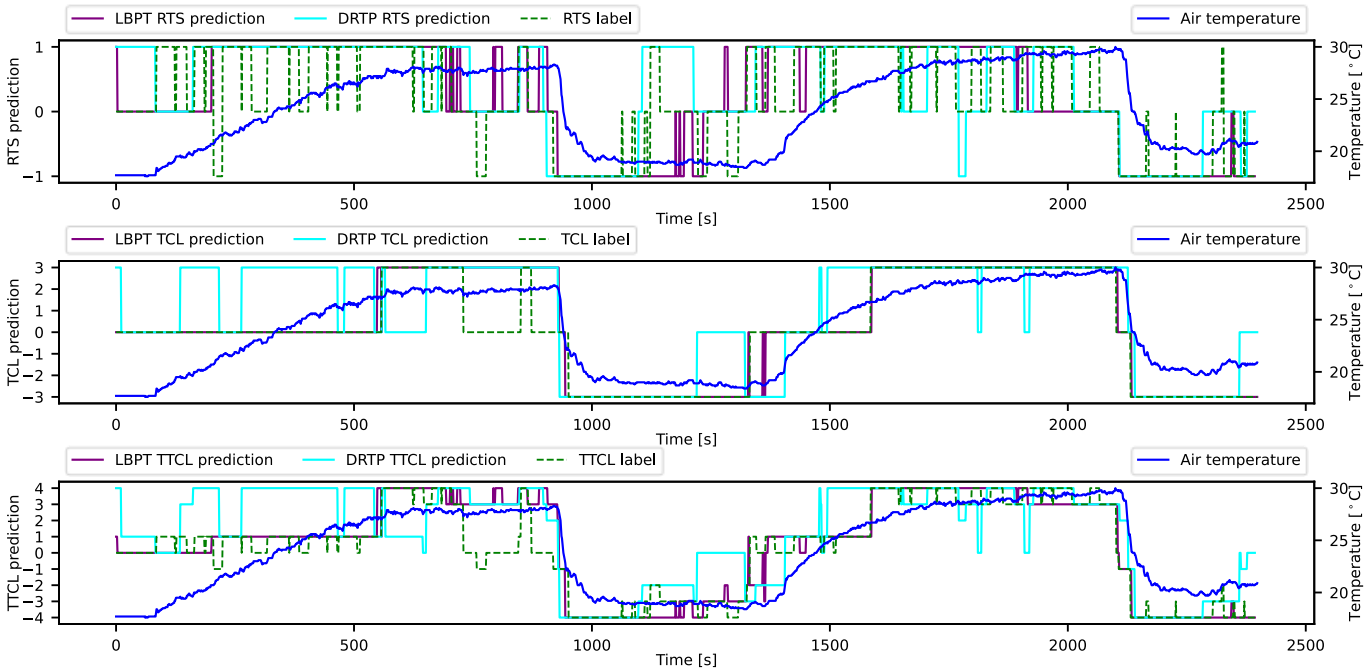

Fig. 9 Prediction of the RTS, TCL, and TTCL (Scenario I & subject 1)

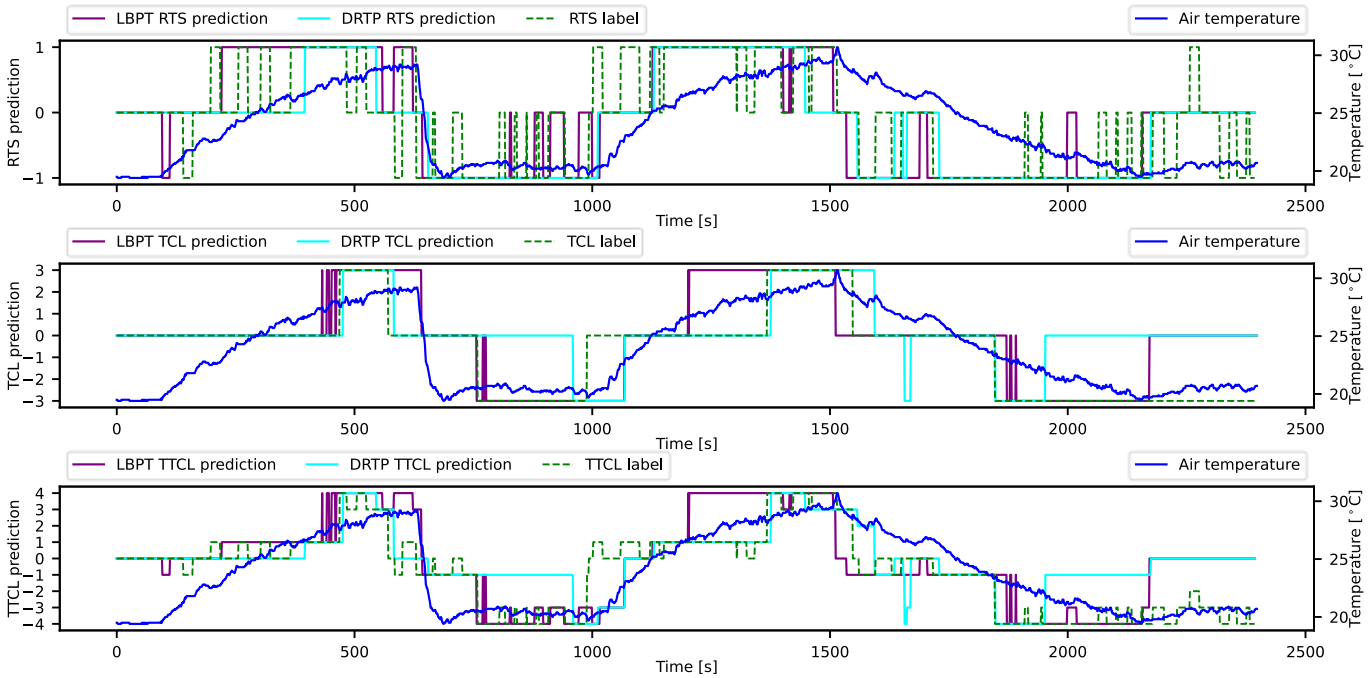

Fig. 10 Prediction of the RTS, TCL, and TTCL (Scenario II & subject 4)

4.2 Thermal discomfort early warning mechanism of the TTCL

Table 1. Mean accuracy of the TTCL predictions in Scenarios I and II using LBPT feature sets or DRTP feature sets.

	Scenario	LBPT	DRTP
TTCL	I	0.57	0.45
	II	0.51	0.41

Table 1 shows the mean accuracy of the TTCL predictions in Scenarios I and II integrated by the RTS predictions and the TCL predictions using LBPT feature sets or DRTP feature sets. The LBPT feature set reached mean accuracies of 0.57 and 0.51 in Scenarios I and II, respectively; the DRTP feature set reached mean accuracies of 0.45 and 0.41 in Scenarios I and II, respectively. Since the number of classes is relatively large (nine), the prediction result is not bad.

Fig. 9 and Fig. 10 show the RTS predictions, TCL predictions, and the integrated TTCL predictions using the LBPT or DRTP feature sets of two subjects from Scenarios I and II, respectively. For instance, in Fig. 9, in the first gradual heating phase, during 400-550 sec, the subject's TCL was still "cozy" while feeling "hotter," the TTCL was mainly "cozy to hot" and was successfully predicted using the LBPT feature set; in Fig. 10, in the gradual cooling phase during 1700-1850 sec, the subject's TCL was still "cozy" after turning on the cooling mode of the air-conditioner and finally reached "cold," the TTCL was mainly "cozy to cold" and was successfully predicted using both LBPT and DRTP feature sets. The significance of the TTCL is that "cozy to hot" and "cozy to cold" TTCLs can generate thermal discomfort early warning mechanisms. In such cases, it is better to turn down the heater/chiller in advance to prevent it from running into "hot" or "cold" TCLs. Not only can thermal comfort be maintained, but energy can also be saved.

Moreover, the significance of the TTCL is that "hot to hot" and "cold to cold" TTCLs can generate thermal discomfort deterioration prevention mechanisms that can prevent occupants' current thermal comfort from deteriorating. For instance, in Fig. 9, in the first gradual heating phase during 1600-1800 sec, the subject's TTCL was mainly "hot to hot" and was successfully predicted using the LBPT feature set; in Fig. 9, in the gradual heating phase during 2150-2250 sec, the subject's TTCL was mainly "cold to cold" and was successfully predicted using both LBPT and DRTP feature sets.

Furthermore, our RTS models have the ability to predict some fine details of the RTS, indicating the validity of the RTS models. For example, in Fig. 9, during 1780-2050 sec, the RTS fine details were well predicted by the DRTP feature set; in Fig. 10, during 850-950 sec, the fine details of the RTS were well predicted by the LBPT feature set.

5. CONCLUSION

This work investigates a novel composite thermal comfort model that simultaneously addresses the occupants' current thermal comfort and the current thermal sensation trend. This pilot study facilitates practical applications for thermal discomfort early warning/deterioration prevention systems and contributes to energy conservation in buildings.

REFERENCE

[1] Buildings – Topics - IEA n.d. https://www.iea.org/topics/buildings (accessed March 20, 2021).

[2] Li D, Menassa CC, Kamat VR. Non-intrusive interpretation of human thermal comfort through analysis of facial infrared thermography. Energy Build 2018;176:246–61.

[3] Ghahramani A, Castro G, Karvigh SA, Becerik-Gerber B. Towards unsupervised learning of thermal comfort using infrared thermography. Appl Energy 2018;211:41–9.

[4] Zhao Y, Zhang H, Arens EA, Zhao Q. Thermal sensation and comfort models for non-uniform and transient environments, part IV: Adaptive neutral setpoints and smoothed whole-body sensation model. Build Environ 2014;72:300–8.

[5] Zhao R. Investigation of transient thermal environments. Build Environ 2007;42:3926–32.

[6] Bolya D, Zhou C, Xiao F, Lee YJ. YOLACT++: Better Real-time Instance Segmentation. IEEE Trans Pattern Anal Mach Intell 2020;PP. https://doi.org/10.1109/TPAMI.2020.3014297.

[7] McInnes L, Healy J, Melville J. UMAP: Uniform Manifold Approximation and Projection for Dimension Reduction 2018.

[8] Bergmeir C, Benítez JM. On the use of cross-validation for time series predictor evaluation. Inf Sci 2012;191:192–213.

